

# Microcapsules with Protein Fibril Reinforced Shells: Effect of Fibril Properties on Mechanical Strength of the Shell

Nam-Phuong K. Humblet-Hua, Erik van der Linden, and Leonard M. C. Sagis\*

Physics and Physical Chemistry of Foods, Department of Agrotechnology and Food Sciences, Wageningen University, Post Office Box 8129, 6700 EV Wageningen, The Netherlands

**ABSTRACT:** In this study, we produced microcapsules using layer-by-layer adsorption of food-grade polyelectrolytes on an emulsion droplet template. We compared the mechanical stability of microcapsules to shells consisting of alternating layers of ovalbumin–high methoxyl pectin (Ova–HMP) complexes and semi-flexible ovalbumin (Ova) fibrils (average contour length,  $L_c \sim 200$  nm), with microcapsules built of alternating layers of lysozyme–high methoxyl pectin (LYS–HMP) complexes and lysozyme (LYS) fibrils. Two types of LYS fibrils were used: short and rod-like ( $L_c \sim 500$  nm) and long and semi-flexible ( $L_c = 1.2\text{--}1.5 \mu\text{m}$ ). At a low number of layers ( $\leq 4$ ), microcapsules from Ova complexes and fibrils were stronger than microcapsules prepared from LYS complexes and fibrils. With an increase of the number of layers, the mechanical stability of microcapsules from LYS–HMP/LYS fibrils increased significantly and capsules were stronger than those prepared from Ova–HMP/Ova fibrils with the same number of layers. The contour length of the LYS fibrils did not have a significant effect on mechanical stability of the LYS–HMP/LYS fibril capsules. The stiffer LYS fibrils produce capsules with a hard but more brittle shell, whereas the semi-flexible Ova fibrils produce capsules with a softer but more stretchable shell. These results show that mechanical properties of this type of capsule can be tuned by varying the flexibility of the protein fibrils.

**KEYWORDS:** *Fibril, encapsulation, layer-by-layer, complex, lysozyme, ovalbumin, pectin*

## INTRODUCTION

Microencapsulation was first introduced in the 1950s by Green and Schleicher.<sup>1</sup> Since then, encapsulation technology has been developed and applied in various fields, including medicine and pharmacy and food and feed.<sup>2</sup> In food products, different components, including aromas, vitamins, probiotics, and enzymes, have been encapsulated,<sup>2–6</sup> using either physical chemical techniques (such as interfacial polymerization, solidification, coacervation, molecular inclusion, gelation, or evaporation) or mechanical techniques (such as spray-drying, spray chilling/cooling, extrusion, or fluidized-bed coating).<sup>2,7–9</sup>

Microencapsulation by layer-by-layer (LbL) assembly, developed in 1991 by Decher et al.,<sup>10–12</sup> is the sequential adsorption of oppositely charged materials on a template to form polyelectrolyte shells.<sup>13–15</sup> It is a simple and inexpensive method to control the shell thickness of the microcapsules<sup>16–18</sup> and the release of encapsulated materials.<sup>18–20</sup>

In this study, we prepared microcapsules by LbL assembly, using oil-in-water emulsion droplets as templates. Surface-active complexes of food-grade proteins and polysaccharides were used as the emulsifier of the template emulsion. After preparation of the template emulsion, alternating layers of fibrillar protein aggregates and protein–polysaccharide complexes were adsorbed to build the shell of the microcapsule.

Protein–polysaccharide complexes have previously been used as emulsion stabilizers and were shown to have high surface activity and the ability to form thick, gel-like, and charged adsorbed layers.<sup>21,22</sup> The mechanical strength of that adsorbed layer, together with the electrostatic and steric repulsion that it induces, is the most important factor influencing the kinetic stability of the oil-in-water emulsion

droplets<sup>13</sup> and will also affect the stability of microcapsules produced with these complexes.

For the complexes, we have chosen ovalbumin (Ova) and lysozyme (LYS), two major egg white proteins, and high methoxyl pectin (HMP). Ova (60–65% of the total proteins in egg white) is available in large quantities and widely used in studies of protein structures and properties.<sup>23</sup> Lysozyme is a well-characterized protein<sup>24</sup> and is a model protein in studying the interaction between proteins and polysaccharides.<sup>25</sup> Pectin is an anionic polysaccharide present in plant cell walls and is commonly used in food products.<sup>25,26</sup> It was found to form complexes with various proteins, such as gelatin,<sup>26</sup> Ova,<sup>27</sup> LYS,<sup>25</sup> and milk proteins.<sup>28–31</sup> The main parameters controlling the formation of stable protein–polysaccharide complexes are pH, ionic strength, charge density, concentration, and protein–polysaccharide ratio.<sup>21,25,32</sup> At chosen pH values (3.5 for Ova and 7 for LYS), the proteins are positively charged, while HMP is negatively charged, resulting in attractive electrostatic interactions to form complexes. A high ionic strength ( $I$ ) will lead to charge screening of the polymers and, hence, affect the formation of complexes.<sup>21,31</sup> Therefore, no extra salts were added to the polymer solutions. We have mixed proteins and HMP at various ratios, and the optimum ratio to obtain stable complexes was determined by visual observation, light scattering, and  $\zeta$  potential distribution measurements.

**Received:** June 7, 2012

**Revised:** August 15, 2012

**Accepted:** August 20, 2012

**Published:** August 20, 2012

The assembly of food-grade proteins, such as milk proteins, Ova, and LYS, into fibrils<sup>33–36</sup> has the potential of broadening the functional properties of these proteins.<sup>37</sup> Fibrils have previously been used to develop microcapsules for encapsulation,<sup>17,18</sup> but a detailed study on how protein fibril properties affect the mechanical stability of the microcapsule has thus far not been performed.

When heated at 80 °C, at pH 2, Ova monomers assemble irreversibly into semi-flexible fibrils with a contour length of a few hundred nanometers and effective diameters of a few nanometers.<sup>38</sup> For LYS, the optimum conditions to form fibrils were at pH 2 and 57 °C.<sup>36</sup> Applying flow during heating was found to influence the morphology of fibrils: higher shearing or stirring rates resulted in shorter fibrils that are more rod-like, whereas at rest or at lower rates, longer semi-flexible fibrils were obtained.<sup>39</sup> In this study, both short and rod-like and long and semi-flexible fibrils were used as encapsulating materials.

From these two types of protein complexes and fibrillar aggregates, two encapsulation systems were developed. System 1 was composed of Ova–HMP complexes and Ova fibrils. The microcapsules of this system were prepared at pH 3.5. At this pH, Ova–HMP complexes have a negative net charge, while Ova fibrils are positively charged. System 2 was composed of LYS–HMP complexes and LYS fibrils. LYS–HMP complexes were adsorbed on the template at pH 7 and negatively charged, and LYS fibrils were adsorbed at pH 5 and, hence, positively charged. Both systems were prepared using simple and standard operations as described in previous studies.<sup>17,18</sup> Using a range of fibrils (short and semi-flexible Ova, short and rod-like LYS, and long and semi-flexible LYS) allowed us to investigate the effect of fibril properties on mechanical stability of the multilayer capsules. The contribution to the mechanical strength by the “complex” layers is not much different for both complexes used.

## MATERIALS AND METHODS

**Materials.** Ova was obtained from Sigma-Aldrich Co., St. Louis, MO (product number A5503), with a purity of at least 98%. LYS from hen egg white was obtained from Sigma-Aldrich Co., St. Louis, MO (3× crystallized, lyophilized powder, product number L6876). HMP was supplied by CP Kelco ApS, Lille Skensved, Denmark (JMH-6, batch number 16849, with a degree of methoxylation of 69.8%). It was characterized in a study by Sagis et al.<sup>17</sup> and has a molecular weight of  $2.7 \times 10^3$  kDa and a radius of gyration of 46 nm.

*n*-Hexadecane was obtained from Merck Schuchardt OHG, Hohenbrunn, Germany (CAS number 544-76-3). (*R*)-(+)-Limonene (97%) was supplied by Sigma-Aldrich Co., St. Louis, MO (CAS number 5989-27-5).

Thioflavin T (ThT) was obtained from Merck Schuchardt OHG, Hohenbrunn, Germany, (CAS number 2390-54-7 and C.I. number 49005). Fluorescein isothiocyanate isomer (FITC) was from Sigma-Aldrich Co., St. Louis, MO (product number F7250-1G and CAS number 3326-32-7).

All other chemicals used were of analytical grade, unless stated otherwise. All solutions were prepared with Millipore water (Millipore Corporation, Billerica, MA). Samples were diluted to the desired concentration (if applicable) with the same buffer or solution used for the primary solutions.

**Preparing Fibrils.** On the basis of results from a study by Veerman et al.,<sup>38</sup> Ova solutions of 5 wt % at pH 2 were heated at 80 °C for 24 h to obtain Ova fibrils.

LYS fibrils with various lengths were prepared as described elsewhere.<sup>39</sup> LYS solutions of 2 wt % at pH 2 were heated at 57 °C in a heating plate (RT15, IKA Werke, Germany) using magnetic stirring bars (20 × 6 mm, VWR International, West Chester, PA). Bottles containing about 18 mL of sample have an inner diameter of

24 mm. Stirring rates of approximately 290 and 550 rpm were applied. At these conditions, two types of fibrils were obtained: long and semi-flexible (called long LYS fibrils) (290 rpm) and short and rod-like (called short LYS fibrils) (550 rpm).

After heating, samples were quenched by cooling immediately on ice and subsequently stored at 4 °C for further investigations. Electron micrographs of the Ova and LYS fibrils were taken using a Philips CM12 electron microscope (Philips, Eindhoven, The Netherlands) [transmission electron microscopy (TEM)].

**Preparing Protein–HMP Complexes.** Protein and HMP solutions (0.1 wt %) were mixed at various protein/HMP ratios ranging from 1:4 to 12:1 (wt/wt). Electron micrographs of the complex coacervates were taken using a Philips CM 12 electron microscope (TEM).

**Methods. Production of Microcapsules.** Microcapsules were prepared as described in a previous study.<sup>18</sup> A 2 wt % emulsion of *n*-hexadecane in 0.1 wt % Ova–HMP complex solution at pH 3.5 or 0.05 wt % LYS–HMP solution at pH 7 was made by mixing with a rotor–stator mixer (Ultra Turrax) using a setting of 13 500 rpm for 90 s for a sample of 20 g of emulsion. Non-adsorbed materials were removed from the emulsion droplets by centrifuging at 100g for 30 min at 20 °C. The concentrated emulsion droplets (“cream” or one-layer microcapsules) were centrifuged again at 750g for 1 min to remove excess solution. After that, the negatively charged droplets were dispersed in a fibril solution of 0.06 wt % Ova fibrils at pH 3.5 or 0.03 wt % LYS fibrils at pH 5. At these pH values, fibrils are positively charged, which allowed assembly driven by electrostatic interaction to form bilayer microcapsules. These bilayer microcapsules were isolated by the same process and dispersed in the same solution used for the first layer. When this process is repeated, additional layers of encapsulating materials can be added (see Figure 1).

Microcapsules for mechanical stability experiments were prepared using an oil mixture of 75 wt % *n*-hexadecane and 25 wt % limonene. All other material concentrations and process conditions were as described above.

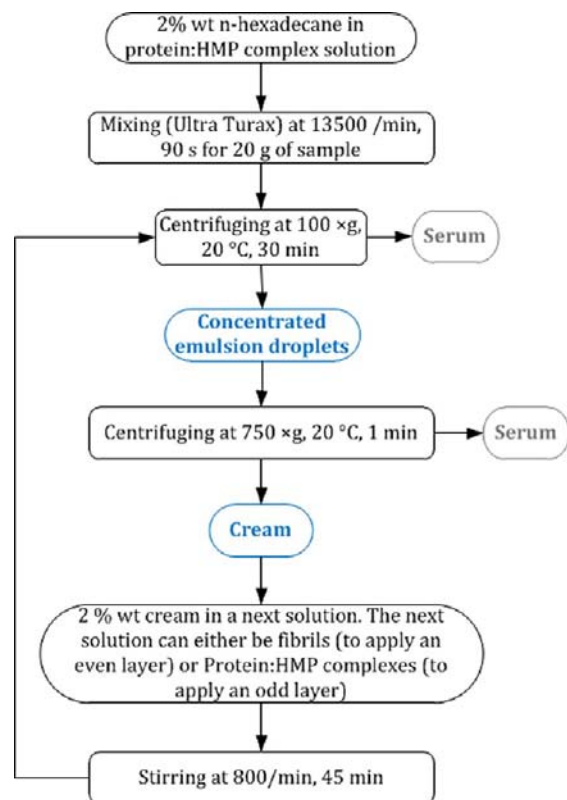
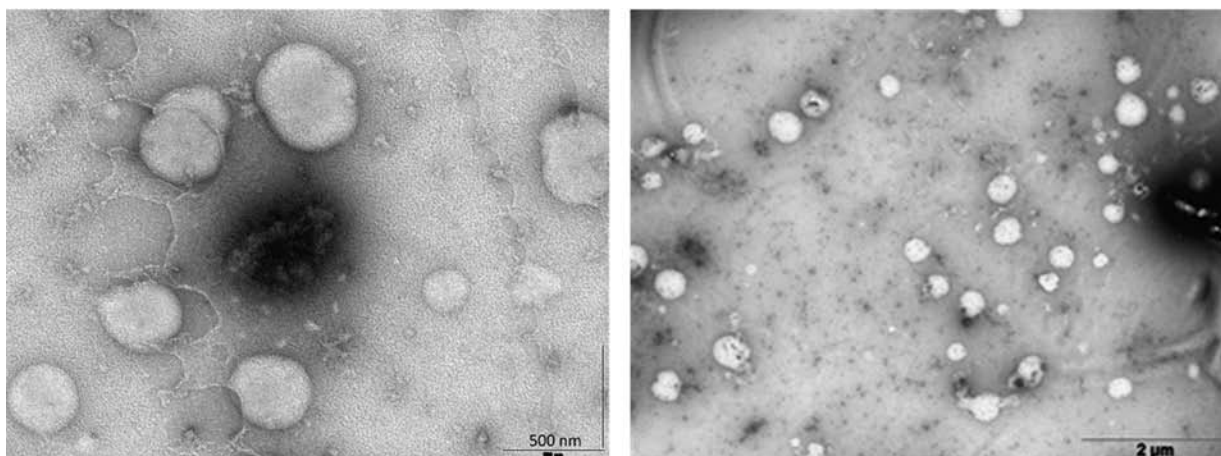


Figure 1. Scheme showing the process of making capsules.

**Table 1.** Average Size (nm) and  $\zeta$  Potential (mV) of Protein–HMP Complexes at Various Ratios (wt/wt)

ratio	Ova–HMP at pH 3.5			LYS–HMP at pH 7		
	Z average [nm]	$\zeta$ potential [mV]	distribution	Z average [nm]	$\zeta$ potential [mV]	distribution
4:1	622	−9.1	one narrow peak	184	−18.7	one narrow peak
2:1	352	−10.5	one narrow peak	180	−19.3	one narrow peak
1:1	269	−11.6	very polydisperse	175	−21.9	very polydisperse
1:2	279	−13.2	very polydisperse	208	−23.5	very polydisperse
1:4	388	−14.4	very polydisperse	301	−23.2	very polydisperse

**Figure 2.** TEM micrographs of 2:1 Ova–HMP complexes (left) and 4:1 LYS–HMP complexes (right). Scale bars represent 500 nm (left) and 2  $\mu$ m (right).

**Light Scattering Measurements.** The size distributions and  $\zeta$  potentials of the protein–HMP complexes were determined using a Zetasizer Nano (Malvern Instruments, Ltd., Worcestershire, U.K.). The size distribution and  $\zeta$  potential of the emulsion droplets and microcapsules were determined using a MasterSizer 2000 and a Zetasizer Nano (Malvern Instruments, Ltd., Worcestershire, U.K.). Creams were redispersed in buffer with the same pH prior to measurements to ensure that the presence of excess polyelectrolytes (not adsorbed on the templates) was minimized. On each sample, three size distribution and five  $\zeta$  potential measurements were performed.

**Confocal Laser Scanning Microscopy (CLSM).** To study the distribution of encapsulating materials on the emulsion droplets, ThT was used to label the fibrils and FITC was used to label either the HMP or the proteins in the complexes.

The dye ThT can have a specific binding to the  $\beta$  sheets in amyloid fibrils<sup>40–44</sup> and is, therefore, widely used to determine the presence of fibrils.<sup>42,45–50</sup> A 3 mM ThT solution at pH 7 was prepared and filtered with Millex-GP filters of 0.22  $\mu$ m pore size. This solution was diluted 50 $\times$  with the fibril solutions.

Covalently labeled HMP was prepared for labeling Ova–HMP complexes. A HMP solution of 2 mg/mL at pH 9 was prepared. To each milliliter of the HMP solution, 1  $\mu$ L of FITC solution [1 mg/mL dimethyl sulfoxide (DMSO)] was added and stirred overnight at 4  $^{\circ}$ C. The excess of FITC was removed by centrifuging samples at approximately 90000g at 15  $^{\circ}$ C for 2 h. The pellet was dissolved in a buffer at pH 3.5. This labeled HMP was then used to make complexes with Ova.

A 2 mg/mL LYS solution was brought to pH 9. Then, 1  $\mu$ L of FITC solution (1 mg/mL DMSO) was added to every milliliter of protein solution. This solution was dialyzed against a phosphate buffer at pH 9 under continuous stirring overnight in a cool room to remove the excessive FITC. Then, labeled LYS solution was diluted with phosphate buffer at pH 7 to mix with the unlabeled HMP solution at pH 7, forming labeled LYS–HMP complexes.

The emulsion droplets were observed under a Zeiss LSM5 Pascal confocal system mounted on an inverted microscope (Zeiss Axiovert

200). The excitation wavelength and emission maxima of ThT are 458 and 482 nm, respectively. For FITC, the excitation wavelength and emission maxima are 488 and 518 nm, respectively. Images were taken with a Leica TCS SP.

**Scanning Electron Microscopy (SEM).** To examine the structure of the shell of the microcapsules with SEM, samples were dried and the oil phase was evaporated using critical point drying (CPD). Dried microcapsules were fixed onto double-stick carbon tape, placed in a dedicated preparation chamber, and sputter-coated with 2 nm tungsten (MED 020, Leica, Vienna, Austria). Samples were analyzed with a field emission scanning electron microscope (Magellan 400, FEI, Eindhoven, The Netherlands) at room temperature at a working distance of 4 mm with SE detection at 2 kV. All images were recorded digitally.

**Cryo-SEM Imaging.** Small drops of samples were placed between two aluminum (HPF) platelets (Wohlwend, Sennwald, Switzerland). Then, all samples were plunge-frozen in liquid ethane with a KF 80 (Leica, Vienna, Austria).

The frozen samples were mounted on a clamping sample holder under LN<sub>2</sub>. After that, they were transferred to a non-dedicated cryo-preparation system (MED 020/VCT 100, Leica, Vienna, Austria) onto a sample stage at −94  $^{\circ}$ C in high vacuum ( $1.3 \times 10^{-6}$  mbar). In this cryo-preparation system, the samples were kept for 3 min, subsequently freeze-fractured, and immediately sputter-coated with 5 nm tungsten. The samples were transferred into the field emission scanning microscope (Magellan 400, FEI, Eindhoven, The Netherlands) on the sample stage at −121  $^{\circ}$ C (vacuum in the sample chamber of  $4 \times 10^{-7}$  mbar).

The analysis was performed at a working distance between 2 and 4 mm with ETD and TLD SE detection at 2 kV and 13 pA. All images were recorded digitally.

**Mechanical Stability.** The mechanical stability of the microcapsules was studied using a standard microscope connected to a temperature-controlled stage (Analysa LTS120, Linkam Scientific Instruments, Ltd., Surrey, U.K.). All samples (prepared at room temperature) were placed on a preheated stage at 90  $^{\circ}$ C, and the heat resistance time, the period for which the microcapsules maintain their spherical shape, was

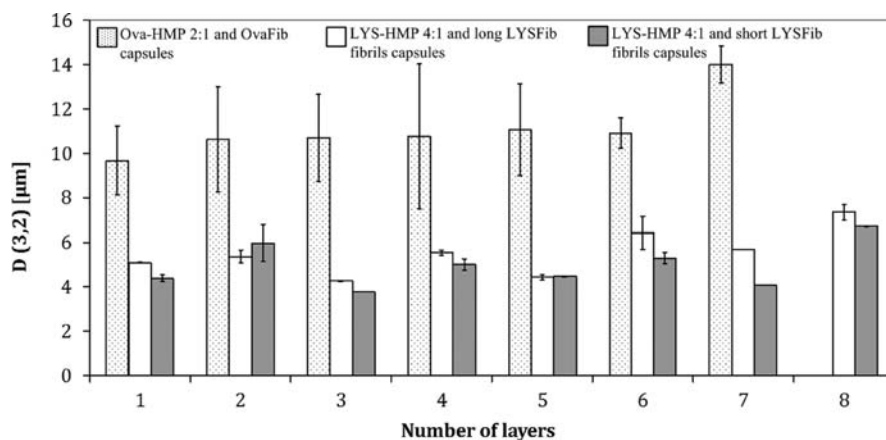


**Figure 3.** Sauter mean diameter  $D(3,2)$  of microcapsules with various numbers of layers. Odd layer numbers represent capsules with an outer layer of protein–HMP complexes. Even layer numbers represent capsules with an outer layer of protein fibrils. The error bars indicate the width of the distribution around the mean diameter values. (First column) Capsules prepared with 2:1 Ova–HMP complexes and Ova fibrils. (Second column) Capsules prepared with 4:1 LYS–HMP complexes and long LYS fibrils. (Third column) Capsules prepared with 4:1 LYS–HMP complexes and short LYS fibrils.

measured. Because the thermal coefficient of the internal oil phase differs from that of the aqueous continuous phase, the temperature increase results in a mechanical strain on the shell. This resistance time is a qualitative measure for the mechanical strength of the shells of capsules. Images of the process were recorded with a digital camera.

## RESULTS AND DISCUSSION

**Complex Formation.** It is well-known that the mixing ratios between protein and polysaccharide have a major effect

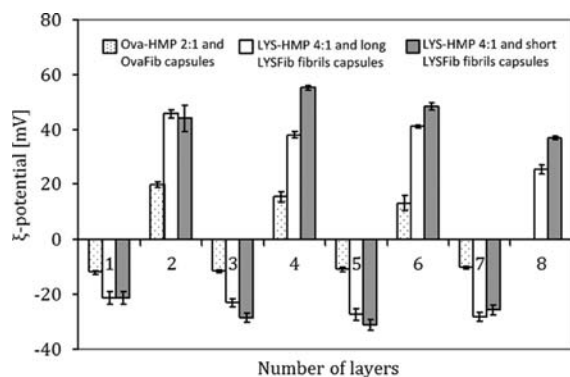


**Figure 4.**  $\zeta$  potential distribution of microcapsules with various layers of encapsulating materials. The bar sequence is similar to that in Figure 3.

on the characteristics of the complexes formed, including their size.<sup>51,52</sup> When the mixture composition contains a high proportion of proteins, very large complexes containing an excess amount of protein will form.<sup>52</sup> For Ova and LYS at the specific conditions used, ratios of protein/HMP of 12:1 and 8:1 (wt/wt) resulted in co-precipitate complexes, leading to phase separation: a dense phase rich in protein and HMP and a dilute phase rich in solvent (results not shown).

**Size and  $\zeta$  Potential Distribution.** The size and  $\zeta$  potential distribution of protein–HMP complexes are summarized in Table 1. Protein/HMP ratios of 4:1 and 2:1 appear to be most suitable for the formation of stable complexes, for both Ova–HMP at pH 3.5 and LYS–HMP at pH 7 mixtures. On the basis of these results, we chose to use a ratio of Ova/HMP equal to 2:1 for the complexes to be used as

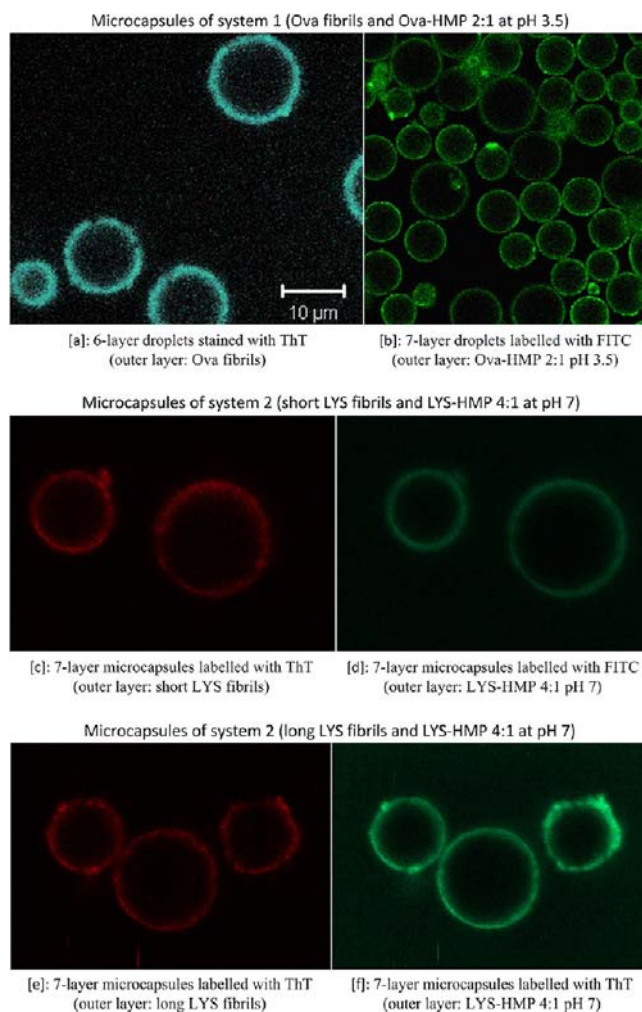


**Figure 5.** CSLM picture showing the material adsorption on microcapsules of system 1 (a and b) and system 2 (c–f): (a) six-layer droplets stained with ThT (outer layer of Ova fibrils), (b) seven-layer droplets labeled with FITC (outer layer of 2:1 Ova–HMP), (c and d) seven-layer microcapsules labeled with ThT (c) and FITC (d) prepared with short LYS fibrils, and (e and f) seven-layer capsules labeled with ThT (e) and FITC (f) prepared with long LYS fibrils.

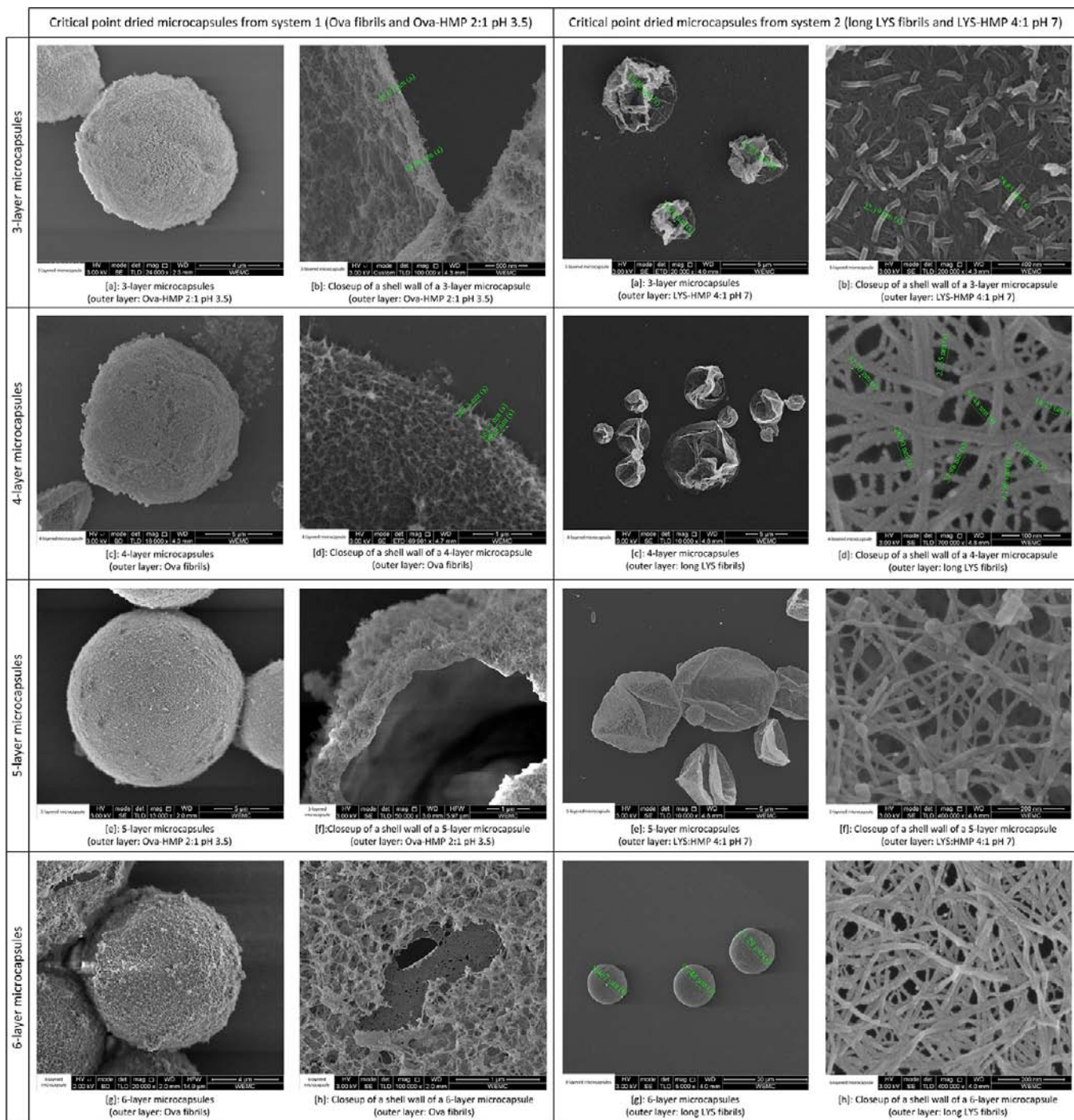


**Figure 6.** SEM pictures showing the structure of the outer layer of (a and b) three-layer, (c and d) four-layer, (e and f) five-layer, and (g and h) six-layer microcapsules. (Left) Microcapsules of system 1 with 2:1 Ova–HMP (odd layers) and Ova fibrils (even layers). (Right) Microcapsules of system 2 with 4:1 LYS–HMP (odd layers) and long LYS fibrils (even layers). The microcapsules were obtained by CPD to remove the inner phase (oil).

the odd layer materials for system 1, because of the smaller size that these have compared to the 4:1 complexes. For LYS–HMP, at both ratios 4:1 and 2:1, complexes were formed with suitable sizes and net charges. The ratio of LYS/HMP equal to 4:1 had, however, a narrower size distribution curve (data not shown). It was therefore chosen as encapsulating material for system 2. Factors determining the characteristics of the complexes include extrinsic factors, such as the mixing ratio, pH, and ionic strength, and intrinsic factors related to the molecules, such as the molecular weight, net charge, and

flexibility of the chains.<sup>22,52,53</sup> Therefore, even though both Ova and LYS are small ellipsoidal molecules with similar dimensions of approximately  $5 \times 5 \times 7$  nm (Ova)<sup>54,55</sup> and  $3 \times 3 \times 4.5$  nm (LYS),<sup>56,57</sup> at the same mixing ratios, Ova–HMP complexes are larger than LYS–HMP complexes (see Table 1).

TEM micrographs (Figure 2) showed that the protein–HMP complexes were roughly spherical, and diameters obtained from the TEM images are in agreement with values measured by light scattering techniques.

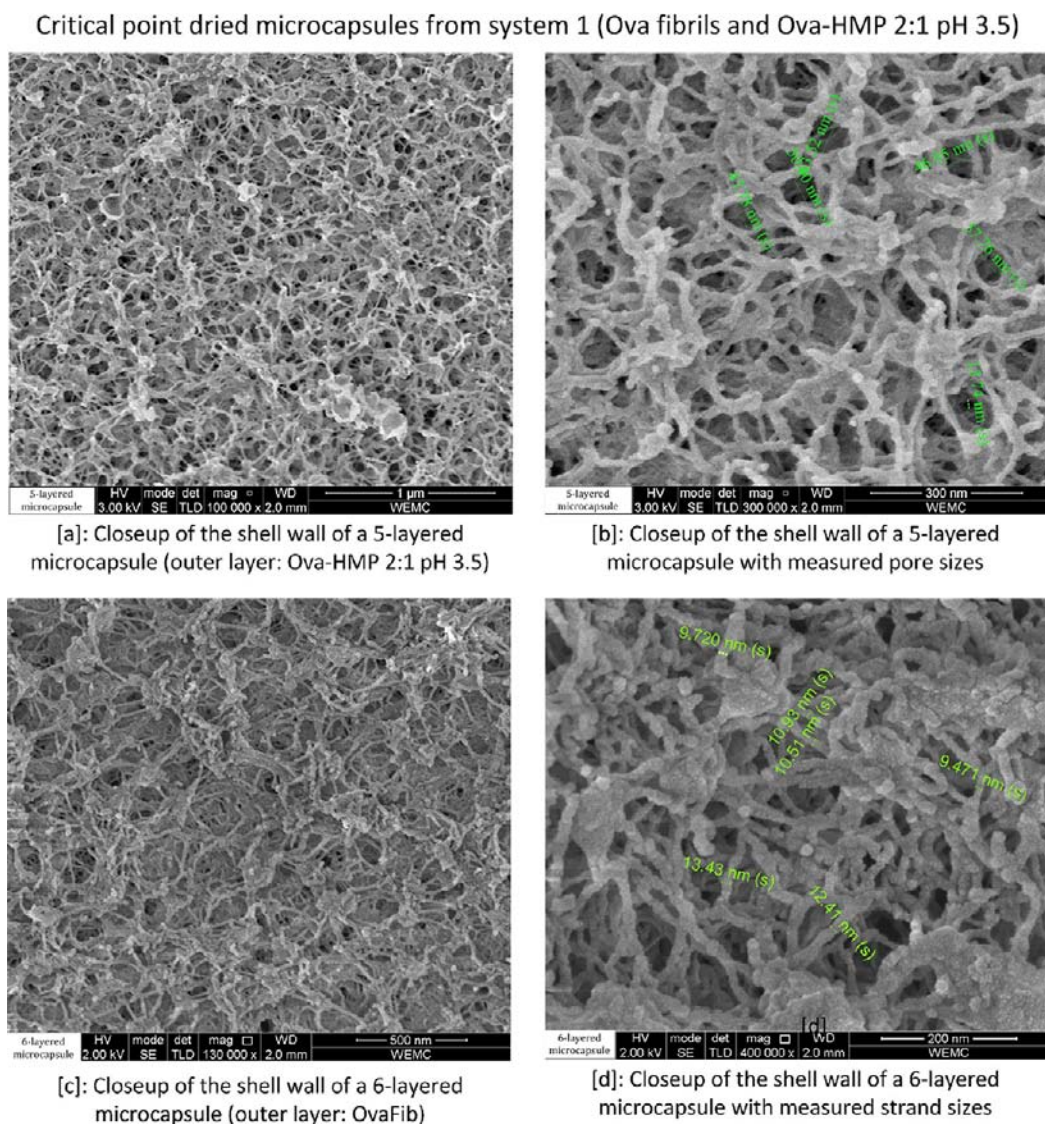


**Figure 7.** SEM pictures showing the structure of the outer layer of (a and b) five-layer microcapsules from system 2 with 2:1 Ova–HMP as the outer layer and (c and d) six-layer microcapsules from system 2 with Ova fibrils as the outer layer. The microcapsules were obtained by CPD to remove the inner phase (oil).

**Growth and Stability.** The growth of the size of the 2:1 Ova–HMP and 4:1 LYS–HMP complexes in time was measured using a Zetasizer Nano (results not shown). After a few hours, the size of the complexes no longer increases and the complexes appear to be stable for at least 4 weeks.

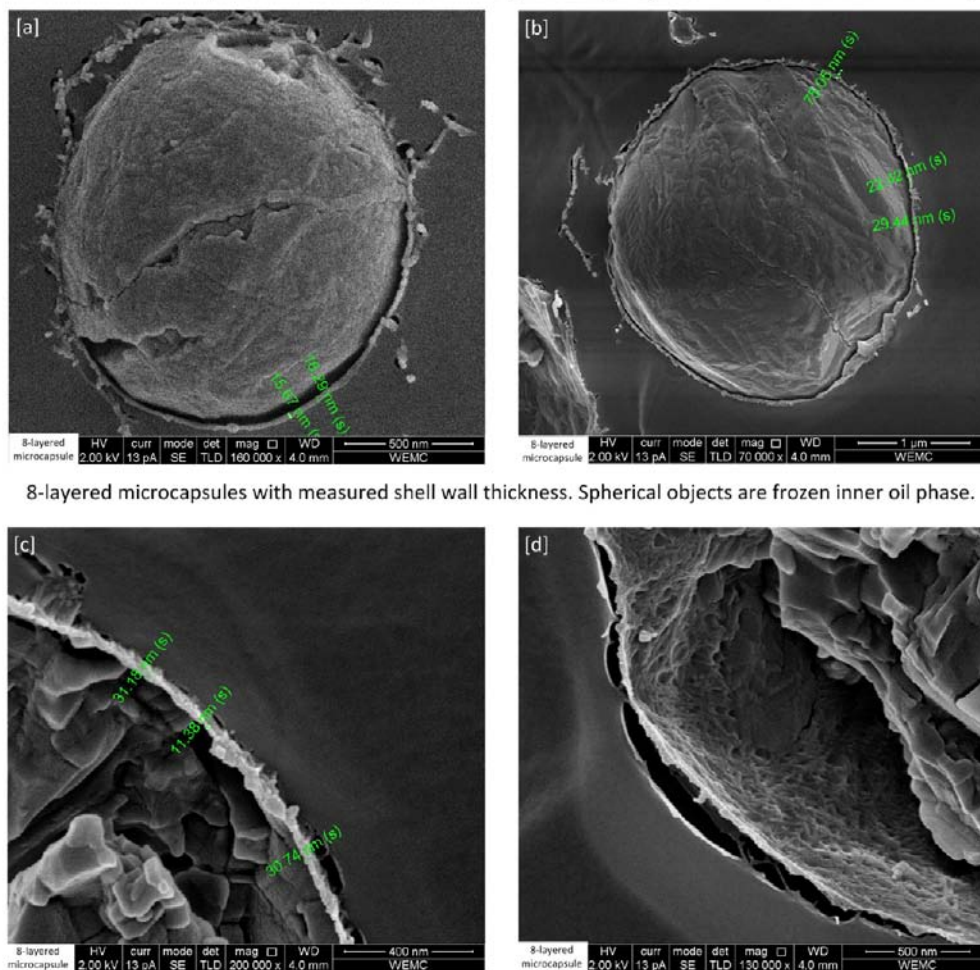
**Microcapsules. Size and  $\zeta$  Potential Distribution.** Light scattering measurements show that microcapsules from either system 1 or 2 are polydisperse (Figure 3). The Sauter mean diameters  $D(3,2)$  of the droplets from system 2 with either long or short LYS fibrils fluctuated between 4 and 6  $\mu\text{m}$ , which was in the same range as microcapsules from a previously studied system with Ova fibril and pure HMP (Figure 3).<sup>18</sup> Droplets from system 1, however, have diameters twice as large as those from the other systems. The size difference is already present in the template emulsion, and this shows that the ability to reduce the amount of free energy required to form droplets is lower for Ova–HMP complexes than for LYS–HMP complexes.<sup>58</sup>

Droplets with an even number of layers (outer layers are fibrils) are larger than those with an odd number of layers

(outer layers are protein–HMP complexes), even when the number of layers is lower. This is particularly true for capsules made with the stiffer LYS fibrils. This fluctuation in diameter could be due to the properties of the encapsulating materials: when stiffer fibrils with a persistence length close to the diameter of the capsules are adsorbed on the surface of the microcapsule, they may not be able to bend sufficiently to adsorb flat on the interface. They will then form a “hairy” layer around the capsule, with parts of the fibrils protruding into the solution. When the “hairy” surface structure of the even-layer droplets was brought into contact with the complexes, it might be smoothed by interacting with the complexes, resulting in slightly smaller odd-layer droplets.

The microcapsules from both systems did not show a significant change in size distribution from one layer to seven or eight layers, even after weeks of storage. This shows that microcapsules made by LbL deposition of protein–HMP complexes and protein fibrils are highly stable over long periods of time.

## Freeze-fractured 8-layered microcapsules from system 2 (long LYS fibrils and LYS-HMP 4:1 pH 7)



8-layered microcapsules with measured shell wall thickness. Spherical objects are frozen inner oil phase.

Closeup of 8-layered microcapsules with measured shell wall thickness (left) and shell wall structure (right).

**Figure 8.** Cryo-SEM pictures showing the structure of eight-layer microcapsules prepared from 4:1 LYS–HMP complexes (odd layers) and long LYS fibrils (even layers). The samples were freeze-fractured, after flash freezing in liquid ethane.

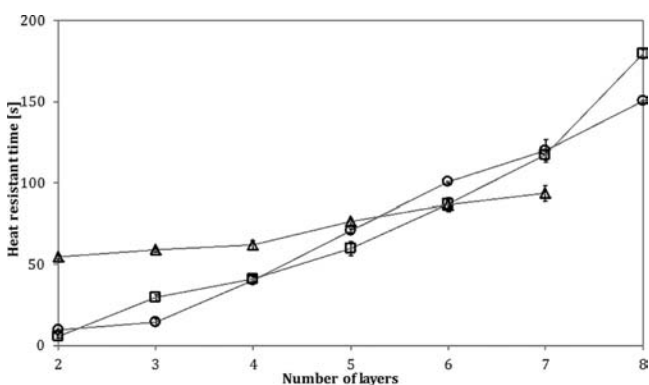


**Figure 9.** Heat resistance time versus number of layers when microcapsules were heated at 90 °C: (Δ) microcapsules from system 1 with 2:1 Ova–HMP and Ova fibrils, (○) microcapsules from system 2 with 4:1 LYS–HMP and long LYS fibrils, and (□) microcapsules from system 2 with 4:1 LYS–HMP and short LYS fibrils.

One of the parameters to monitor the adsorption of oppositely charged polyelectrolytes on microcapsules in the LbL process is to measure their surface net charge. LbL adsorption based on electrostatic interaction leads to a surface charge reversion;<sup>14,16,59,60</sup> i.e., the final outer layer normally

determines the interfacial net charge.<sup>13,15</sup> The  $\zeta$  potential distribution of microcapsules switches from negative (odd number of layers with protein–HMP complexes as outer layers) to positive (even number of layers with protein fibrils as the outer layer), confirming the LbL adsorption of materials (Figure 4). There is a slight decrease in the positive charges as a function of the number of (even) layers, while the charges of odd-layer droplets were stable or increased as the layer number increased.

**Capsule Morphology.** Results from the imaging of the microcapsules with CSLM are shown in Figure 5.

ThT adsorbs to the  $\beta$  sheets formed in amyloid fibril.<sup>42,43</sup> Therefore, it is used to observe the adsorption of fibrils on the microcapsules. FITC was bound covalently to one component of the protein–HMP complexes. The fluorescence signals (Figure 5) confirm the adsorption of alternating layers of fibrils and complexes on the emulsion droplet templates, in line with the results of  $\zeta$  potential measurements. These signals also visualize the inhomogeneity of the shells of the microcapsules. The inhomogeneous distribution of encapsulating materials was observed for both materials: complexes and fibrils. Because the excitation maxima of ThT (482 nm) and FITC (518 nm) are close to each other, it was not possible to observe their signals

at the same time to be able to visualize their interaction in the shell.

The results from the analysis of the capsules with SEM and cryo-SEM are shown in Figure 6 to Figure 8. Microcapsules of both systems were dried by the same CPD method. Because SEM pictures of microcapsules with short LYS fibrils were quite similar in surface structure to those with long LYS fibrils, they were not included in Figure 6. Apparently, the difference in size and flexibility between these two types of LYS fibrils did not have a significant effect on the structure of the shell of the microcapsules.

Figure 6 shows that microcapsules prepared with 2:1 Ova–HMP and Ova fibrils were more resistant to the drying process than those prepared with 4:1 LYS–HMP and LYS fibrils. The shell structure of microcapsules from system 1 was also denser than that of microcapsules from system 2.

In system 1, the “hairy” structure of microcapsules with an even number of layers could clearly be observed. In the SEM picture of a four-layer microcapsule, it can be seen that adsorbed Ova fibrils were protruding from the surface. When the next layer of material was adsorbed, the shell was smoothened. Unfortunately, that phenomenon could not be observed in system 2, because of collapsing of the microcapsules after drying, for capsules with five or fewer layers. For system 2, the images clearly indicate that the strength of the microcapsule shell increases when the number of adsorbed layers increases. Whereas shells with five or fewer layers have all collapsed after drying, capsules with six or more layers remain spherical. Close-up pictures of the microcapsules of systems 1 and 2 with long LYS fibrils (Figure 6) and system 1 (Figure 7) show that their shells are quite inhomogeneous and consist of layers of networks of fibrils with relatively large pores and a considerable number of defects. Increasing the number of layers does seem to decrease the sizes of pores and decrease the number of defects. The thicknesses of the strands in the network are similar to the diameter of a single protein fibril.

The structure of microcapsule shells was also studied with cryo-SEM. In Figure 8d, we see that the network structure of the shell in a frozen state is similar to the structure observed in dried microcapsules. This shows that the preparation steps (CPD for SEM and flash freezing for cryo-SEM) had little effect on the structure of the shell. From panels a–c of Figure 8, we can obtain an indication of the thickness of the shells of the microcapsules. We see that eight-layer shells have a thickness that varies from less than 20 nm to more than 70 nm, confirming the inhomogeneity of the microcapsule shells observed in CLSM and SEM pictures of dried microcapsules.

**Mechanical Stability.** In this experiment, we obtained a qualitative measure for the mechanical strength of the capsule shells by exposing them to a high temperature (90 °C) and measuring the time for which the capsules remain spherical, as observed under the microscope. In the SEM experiments, we saw little difference in the structure of the shell of capsules made with either short or long LYS fibrils. These findings are confirmed by the heat stability measurements, where we do not find a significant difference in the dependence of the heat resistance time upon the number of layers (Figure 9).

From the results of these measurements, it can be seen that, in systems produced with LYS–HMP complexes and LYS fibrils, no significant difference was observed in mechanical stability between capsules produced with short and rod-like fibrils and capsules produced with long and semi-flexible fibrils. The slope of the curves in Figure 9 is, however, considerably

steeper for the Ova system than for LYS systems. In the Ova system, increasing the number of layers from two to seven increased the heat resistance time (when heating at 90 °C) by approximately a factor 1.5, whereas in LYS systems, that factor was about 15. Capsules prepared with semi-flexible Ova fibrils and Ova–HMP complexes were stronger than systems based on LYS, for capsules with four or fewer layers. The short and semi-flexible Ova fibrils combined with the larger 2:1 Ova–HMP complex (a factor of 2 larger than 4:1 LYS–HMP complex) apparently result in a more compact and stretchable shell, whereas the stiffer LYS fibrils result in more inhomogeneous and more brittle shells.

The differences in mechanical strength between these systems were also reflected in the SEM images of critical point dried capsules where three-layer capsules prepared with Ova fibrils and Ova–HMP remained intact, whereas only the six-layer capsules prepared with LYS fibrils and LYS–HMP could retain their spherical shape. These findings show that we can tune the mechanical properties of the shell of this type of multilayer capsule by changing the properties of the fibrils.

## AUTHOR INFORMATION

### Corresponding Author

\*Telephone: +31-317-485023. Fax: +31-317-483669. E-mail: leonard.sagis@wur.nl.

### Funding

The work was partly supported by the European Commission within the Project “Controlled Release” (NMP3-CT-2006-033339).

### Notes

The authors declare no competing financial interest.

## ACKNOWLEDGMENTS

The authors thank H. Baptist (Food Physics Group), A. van Aelst (Wageningen Electron Microscopy Centre), and N. de Ruijter and H. Kieft (Wageningen Light Microscopy Centre) from Wageningen University for their assistance with the microscopy experiments.

## ABBREVIATIONS USED

CLSM, confocal laser scanning microscopy; FITC, fluorescein isothiocyanate isomer; HMP, high methoxyl pectin; LYS, lysozyme; LYS–HMP, lysozyme–high methoxyl pectin; Ova, ovalbumin; Ova–HMP, ovalbumin–high methoxyl pectin; SEM, scanning electron microscopy; TEM, transmission electron microscopy; ThT, thioflavin T

## REFERENCES

- (1) Green, B. K.; Schleicher, L. Pressure responsive record materials. U.S. Patents 2,730,456 and 2,730,457, 1956.
- (2) Madene, A.; Jacquot, M.; Scher, J.; Desobry, S. Flavour encapsulation and controlled release: A review. *Int. J. Food Sci. Technol.* **2006**, *41*, 1–21.
- (3) Dziezak, J. D. Microencapsulation and encapsulated ingredients. *Food Technol.* **1988**, *42*, 136–151.
- (4) Schrooyen, P. M. M.; van der Meer, R.; Kruif, C. G. D. Microencapsulation: Its application in nutrition. *Proc. Nutr. Soc.* **2001**, *60*, 475–479.
- (5) Jackson, L. S.; Lee, K. Microencapsulation and the food industry. *Lebensm.-Wiss. Technol.* **1991**, *24*, 289–297.
- (6) Shahidi, F.; Han, X.-Q. Encapsulation of food ingredients. *Crit. Rev. Food Sci.* **1993**, *33*, 501–547.



- (7) Gibbs, B. F.; Kermasha, S.; Allie, I.; Mulligan, C. N. Encapsulation in the food industry: a review. *Int. J. Food Sci. Nutr.* **1999**, *50*, 213–224.
- (8) Dewettinck, K.; Huyghebaert, A. Fluidized bed coating in food technology. *Trends Food Sci. Technol.* **1999**, *10*, 163–168.
- (9) Rosenberg, M.; Sheu, T. Y. Microencapsulation of volatiles by spray-drying in whey protein-based wall systems. *Int. Dairy J.* **1996**, *6*, 273–284.
- (10) Decher, G.; Hong, J. D. Buildup of ultrathin multilayer films by a self-assembly process: I. Consecutive adsorption of anionic and cationic bipolar amphiphiles. *Makromol. Chem., Macromol. Symp.* **1991**, *46*, 321–327.
- (11) Decher, G.; Hong, J. D. Buildup of ultrathin multilayer films by a self-assembly process: II. Consecutive adsorption of anionic and cationic bipolar amphiphiles and polyelectrolytes on charged surfaces. *Ber. Bunsen-Ges.* **1991**, *95*, 1430–1434.
- (12) Decher, G.; Hong, J. D.; Schmitt, J. Buildup of ultrathin multilayer films by a self-assembly process: III. Consecutively alternating adsorption of anionic and cationic polyelectrolytes on charged surfaces. *Thin Solid Films* **1992**, *210–211*, 831–835.
- (13) McClements, D. J. Theoretical analysis of factors affecting the formation and stability of multilayered colloidal dispersions. *Langmuir* **2005**, *21*, 9777–9785.
- (14) Ai, H.; Jones, S. A.; Lvov, Y. M. Biomedical applications of electrostatic layer-by-layer nano-assembly of polymers, enzymes, and nanoparticles. *Cell Biochem. Biophys.* **2003**, *39*, 23–43.
- (15) Decher, G. In *Multilayer Thin Films: Sequential Assembly of Nanocomposite Materials*; Decher, G., Schlenoff, J. B., Eds.; Wiley-VCH: Weinheim, Germany, 2003; pp 1–46.
- (16) Peyratout, C. S.; Dähne, L. Tailor-made polyelectrolyte microcapsules: From multilayers to smart containers. *Angew. Chem., Int. Ed.* **2004**, *43*, 3762–3783.
- (17) Sagis, L. M. C.; de Ruiter, R.; Miranda, F. J. R.; de Ruiter, J.; Schroen, K.; van Aelst, A. C.; Kieft, H.; Boom, R.; van der Linden, E. Polymer microcapsules with a fiber-reinforced nanocomposite shell. *Langmuir* **2008**, *24*, 1608–1612.
- (18) Humblet-Hua, K. N. P.; Scheltens, G.; van der Linden, E.; Sagis, L. M. C. Encapsulation systems based on ovalbumin fibrils and high methoxyl pectin. *Food Hydrocolloids* **2011**, *25*, 569–576.
- (19) Mauser, T.; Déjugnat, C.; Sukhorukov, G. B. Balance of hydrophobic and electrostatic forces in the pH response of weak polyelectrolyte capsules. *J. Phys. Chem. B* **2006**, *110*, 20246–20253.
- (20) Wang, C.; Ye, S.; Sun, Q.; He, C.; Ye, W.; Liu, X.; Tong, Z. Microcapsules for controlled release fabricated via layer-by-layer self-assembly of polyelectrolytes. *J. Exp. Nanosci.* **2008**, *3*, 133–145.
- (21) Ye, A. Complexation between milk proteins and polysaccharides via electrostatic interaction: Principles and applications—A review. *Int. J. Food Sci. Technol.* **2008**, *43*, 406–415.
- (22) Schmitt, C.; Turgeon, S. L. Protein/polysaccharide complexes and coacervates in food systems. *Adv. Colloid Interface Sci.* **2011**, *167*, 63–70.
- (23) Huntington, J. A.; Stein, P. E. Structure and properties of ovalbumin. *J. Chromatogr., B: Biomed. Sci. Appl.* **2001**, *756*, 189–198.
- (24) Imoto, T.; Johnson, L. N.; North, A. C. T.; Phillips, D. C.; Rupley, J. A. 21 vertebrate lysozymes. In *The Enzymes*; Paul, D. B., Ed.; Academic Press: New York, 1972; Vol. 7, pp 665–868.
- (25) Schmidt, I.; Cousin, F.; Huchon, C.; Boué, F.; Axelos, M. A. V. Spatial structure and composition of polysaccharide–protein complexes from small angle neutron scattering. *Biomacromolecules* **2009**, *10*, 1346–1357.
- (26) Dalev, P. G.; Simeonova, L. S. Emulsifying properties of protein–pectin complexes and their use in oil-containing foodstuffs. *J. Sci. Food Agric.* **1995**, *68*, 203–206.
- (27) Kudryashova, E. V.; Visser, A. J. W. G.; van Hoek, A.; de Jongh, H. H. J. Molecular details of ovalbumin–pectin complexes at the air/water interface: A spectroscopic study. *Langmuir* **2007**, *23*, 7942–7950.
- (28) Zaleska, H.; Mazurkiewicz, J.; Tomasik, P.; Bączkiewicz, M. Electrochemical synthesis of polysaccharide–protein complexes. Part 2. Apple pectin–casein complexes. *Nahrung* **1999**, *43*, 278–283.
- (29) Benichou, A.; Aserin, A.; Garti, N. Protein–polysaccharide interactions for stabilization of food emulsions. *J. Dispersion Sci. Technol.* **2002**, *23*, 93–123.
- (30) Girard, M.; Turgeon, S. L.; Gauthier, S. F. Thermodynamic parameters of  $\beta$ -lactoglobulin–pectin complexes assessed by isothermal titration calorimetry. *J. Agric. Food Chem.* **2003**, *51*, 4450–4455.
- (31) Weinbreck, F.; de Vries, R.; Schrooyen, P.; de Kruif, C. G. Complex coacervation of whey proteins and gum arabic. *Biomacromolecules* **2003**, *4*, 293–303.
- (32) Cooper, C. L.; Dubin, P. L.; Kayitmazer, A. B.; Turksen, S. Polyelectrolyte–protein complexes. *Curr. Opin. Colloid Interface Sci.* **2005**, *10*, 52–78.
- (33) Krebs, M. R. H.; Wilkins, D. K.; Chung, E. W.; Pitkeathly, M. C.; Chamberlain, A. K.; Zurdo, J.; Robinson, C.; Dobson, C. M. Formation and seeding of amyloid fibrils from wild-type hen lysozyme and a peptide fragment from the  $\beta$ -domain. *J. Mol. Biol.* **2000**, *300*, 541–549.
- (34) Goda, S.; Takano, K.; Yamagata, Y.; Nagata, R.; Akutsu, H.; Maki, S.; Namba, K.; Yutani, K. Amyloid protofilament formation of hen egg lysozyme in highly concentrated ethanol solution. *Protein Sci.* **2000**, *9*, 369–375.
- (35) Cao, A.; Hu, D.; Lai, L. Formation of amyloid fibrils from fully reduced hen egg white lysozyme. *Protein Sci.* **2004**, *13*, 319–324.
- (36) Arnaudov, L. N.; de Vries, R. Thermally induced fibrillar aggregation of hen egg white lysozyme. *Biophys. J.* **2005**, *88*, 515–526.
- (37) Akkermans, C.; Venema, P.; Rogers, S. S.; van der Goot, A. J.; Boom, R. M.; van der Linden, E. Shear pulses nucleate fibril aggregation. *Food Biophys.* **2006**, *1*, 144–150.
- (38) Veerman, C.; de Schiffart, G.; Sagis, L. M. C.; van der Linden, E. Irreversible self-assembly of ovalbumin into fibrils and the resulting network rheology. *Int. J. Biol. Macromol.* **2003**, *33*, 121–127.
- (39) Humblet-Hua, N.-P.; Sagis, L. M. C.; van der Linden, E. Effects of flow on hen egg white lysozyme (HEWL) fibril formation: Length distribution, flexibility, and kinetics. *J. Agric. Food Chem.* **2008**, *56*, 11875–11882.
- (40) Nilsson, M. R. Techniques to study amyloid fibril formation in vitro. *Methods* **2004**, *34*, 151–160.
- (41) Azakami, H.; Mukai, A.; Kato, A. Role of amyloid type cross  $\beta$ -structure in the formation of soluble aggregate and gel in heat-induced ovalbumin. *J. Agric. Food Chem.* **2005**, *53*, 1254–1257.
- (42) Krebs, M. R. H.; Bromley, E. H. C.; Donald, A. M. The binding of thioflavin-T to amyloid fibrils: Localisation and implications. *J. Struct. Biol.* **2005**, *149*, 30–37.
- (43) Bolder, S. G.; Sagis, L. M. C.; Venema, P.; van der Linden, E. Thioflavin T and birefringence assays to determine the conversion of proteins into fibrils. *Langmuir* **2007**, *23*, 4144–4147.
- (44) Khodarahmi, R.; Soori, H.; Karimi, S. A. Chaperone-like activity of heme group against amyloid-like fibril formation by hen egg ovalbumin: Possible mechanism of action. *Int. J. Biol. Macromol.* **2009**, *44*, 98–106.
- (45) Bromley, E. H. C.; Krebs, M. R. H.; Donald, A. M. Aggregation across the lengthscales in  $\beta$ -lactoglobulin. *Faraday Discuss.* **2005**, *128*, 13–27.
- (46) Naiki, H.; Higuchi, K.; Hosokawa, M.; Takeda, T. Fluorometric determination of amyloid fibrils in vitro using the fluorescent dye, thioflavine T. *Anal. Biochem.* **1989**, *177*, 244–249.
- (47) LeVine, H., III; Ronald, W. Quantification of  $\beta$ -sheet amyloid fibril structures with thioflavin T. In *Method Enzymology*; Academic Press: New York, 1999; Vol. 309, pp 274–284.
- (48) Nielsen, L.; Khurana, R.; Coats, A.; Frokjaer, S.; Brange, J.; Vyas, S.; Uversky, V. N.; Fink, A. L. Effect of environmental factors on the kinetics of insulin fibril formation: Elucidation of the molecular mechanism. *Biochemistry* **2001**, *40*, 6036–6046.
- (49) Groenning, M.; Norrman, M.; Flink, J. M.; van de Weert, M.; Bukrinsky, J. T.; Schluckebier, G.; Frokjaer, S. Binding mode of Thioflavin T in insulin amyloid fibrils. *J. Struct. Biol.* **2007**, *159*, 483–497.

(50) Kroes-Nijboer, A.; Lubbersen, Y. S.; Venema, P.; van der Linden, E. Thioflavin T fluorescence assay for  $\beta$ -lactoglobulin fibrils hindered by DAPH. *J. Struct. Biol.* **2009**, *165*, 140–145.

(51) Weinbreck, F.; Nieuwenhuijse, H.; Robijn, G. W.; de Kruijff, C. G. Complexation of whey proteins with carrageenan. *J. Agric. Food Chem.* **2004**, *52*, 3550–3555.

(52) Turgeon, S. L.; Laneuville, S. I. Protein + polysaccharide coacervates and complexes: From scientific background to their application as functional ingredients in food products. In *Modern Biopolymer Science*; Kasapis, S., Norton, I. T., Ubbink, J. B., Eds.; Academic Press: New York, 2009; Chapter 11, pp 327–363.

(53) Turgeon, S. L.; Schmitt, C.; Sanchez, C. Protein–polysaccharide complexes and coacervates. *Curr. Opin. Colloid Interface Sci.* **2007**, *12*, 166–178.

(54) Sagis, L. M. C.; Veerman, C.; van der Linden, E. Mesoscopic properties of semiflexible amyloid fibrils. *Langmuir* **2004**, *20*, 924–927.

(55) Beverung, C. J.; Radke, C. J.; Blanch, H. W. Protein adsorption at the oil/water interface: Characterization of adsorption kinetics by dynamic interfacial tension measurements. *Biophys. Chem.* **1999**, *81*, 59–80.

(56) Broide, M. L.; Tominc, T. M.; Saxowsky, M. D. Using phase transitions to investigate the effect of salts on protein interactions. *Phys. Rev. E: Stat. Phys., Plasmas, Fluids, Relat. Interdiscip. Top.* **1996**, *53*, 6325–6335.

(57) Cardinaux, F.; Stradner, A.; Schurtenberger, P.; Sciortino, F.; Zaccarelli, E. Modeling equilibrium clusters in lysozyme solution. *EPL* **2007**, *77*, 48004.

(58) McClements, D. J. Biopolymers in food emulsions. In *Modern Biopolymer Science*; Stefan, K., Norton, I. T., Ubbink, J. B., Eds.; Academic Press: New York, 2009; Chapter 4, pp 129–166.

(59) Schönhoff, M. Layered polyelectrolyte complexes: Physics of formation and molecular properties. *J. Phys.: Condens. Matter* **2003**, R1781.

(60) Dickinson, E. Mixed biopolymers at interfaces: Competitive adsorption and multilayer structures. *Food Hydrocolloids* **2011**, *25*, 1966–1983.